IIETA International Information and Engineering Technology Association
Advancing the World of Information and Engineering

Mathematical Modelling of Engineering Problems
Vol. 12, No. 10, October, 2025, pp. 3376-3384
Journal homepage: http://iieta.org/journals/mmep

Influence of Joule Heating and Heat Source on Radiative Magnetohydrodynamic Flow Through Parallel Porous Plates with Oscillatory Suction and Injection

Mustafa Abdullah[1*], Feras Naimat[2], B. Rushi Kumar[3]

[1] Robotics and Artificial Intelligence Engineering Department, Faculty of Engineering, Al-Ahliyya Amman University, Amman 19328, Jordan
[2] Medical Engineering Department, Faculty of Engineering, Al-Ahliyya Amman University, Amman 19328, Jordan
[3] Department of Mathematics, School of Advanced Sciences, Vellore Institute of Technology, Vellore 632014, India

Corresponding Author Email: mrashied@ammanu.edu.jo

https://doi.org/10.18280/mmep.121004

Received: 14 May 2025
Revised: 19 August 2025
Accepted: 25 August 2025
Available online: 31 October 2025

Keywords:
MHD, porous plates, viscous dissipation, Joule heating, oscillatory suction

ABSTRACT

This study investigates the combined effects of Joule heating, viscous dissipation, and oscillatory suction/injection on radiative magnetohydrodynamic (MHD) flow between two infinite parallel porous plates. Unlike previous studies that examine these factors individually, this research presents a comprehensive analysis incorporating all these effects simultaneously under unique boundary conditions—specifically a moving upper plate and a fixed pressure gradient. The governing momentum and energy equations are solved via an implicit finite difference method, and the solutions are validated using an analytical eigenfunction expansion technique for special cases. The influences of key parameters—including magnetic field strength, radiation intensity, heat generation rate, suction frequency, and thermal diffusivity—on the velocity and temperature profiles are examined and discussed. The results provide insights for novel insights relevant to thermal systems involving conductive fluids in porous channels.

1. INTRODUCTION

The effect of many different factors on magnetohydrodynamic (MHD) systems and in various conditions has been studied in the past decades. MHD flow has many different applications, like MHD pumps, MHD generators, accelerators, and many others. Among these studies, permeable plates were addressed with the influence of various factors. A free convective (FC) flow between vertical porous parallels is caused due to the repeated heating of the plates with porous features, as studied by Jha and Ajibade [1], where the flow is considered completely developed and steady. The unstable magnetohydrodynamic flow of a viscous incompressible non-Newtonian Casson fluid between 2-plates with porous features in parallel nonconducting in a medium with porous features with a hall effect and uniform injection and suction have been worked by Wahiduzzaman et al. [2]. Palani and Gnanambigai [3] worked out the outcome of magnetic field (MF) and thermal radiation (TR) on FC flow on a moving vertical plate with porous characteristics. The flow of the fluid and heat transfer of a pseudo-plastic non-Newtonian NF over a porous surface has been worked out by Maleki et al. [4], considering suction and injection. The impacts of viscoelastic parameters and viscous dissipation (VD) on the MHD- FC flow of a viscoelastic fluid on a porous surface accelerated with radiation were demonstrated by Fagbade et al. [5]. The transient flow of MHD-FC of an incompressible medium over a porous, periodically moving plate with slippage at the surface was investigated by Nandi and Kumbhakar [6] in the existence of rotation and Hall current. The effects of permeability of porous materials and injection/suction with VD on an incompressible medium passing through a vertical porous channel were theoretically investigated [7]. A systematic solution of transferring heat and a transient flow of magnetohydrodynamic of a liquid with viscous on a porous oscillating vertical plate exists in TR [8]. Ahammad et al. [9] explained a study of the effectiveness of magnetohydrodynamic and suction velocity in transferring heat in a porous fluid neighboring a vertical porous plate. Loganathan and Elamparithi [10] explained the heat transfer and flow in MHD mixed convection into an infinite vertical porous with the Dufour effect.

Moreover, the effectuality of Joule heating (JH) and VD on many MHD systems has been studied. The effectiveness of MHD-FC flow across a vertical plate with heat conduction, and JH was investigated [11]. Abo-Eldahab and El Aziz [12] examine the effectiveness of JH and VD on MHD- FC flow across a vertical plate in the existence of both the influence of Hall and ion-slip currents. The effect of JH and VD on the momentum and thermal transfer of the flow of MHD across an inclined plate was studied [13]. Jaber studied the impacts of VD and JH on MHD-FC flow across a stretched isothermal vertical sheet [14]. Shamshuddin and Satya Narayana [15] observed the effectuality of JH and VD on the MHD squeezing flow between two Riga plates. Sharma and Gandhi [16] studied the transient magnetohydrodynamics heat transfer for a viscous incompressible fluid via a vertical stretching surface under the impact of velocity slip in the existence of heat

absorption. Pal and Talukdar [17] studied the influences of convection and TR on an unstable MHD in transferring heat for a viscous liquid passing a vertically moving plate. The impacts of JH and non-linear TR on magnetohydrodynamics viscoelastic flow of NF (nanofluid) due to stretching in the surface in lateral directions were investigated [18]. The effectiveness of nonlinear convection, Joule dissipation, and viscous flow on an incompressible fluid's velocity profile and temperature passing a flat plate during an oscillatory motion was investigated [19]. Abdullah theoretically worked out the impact of the periodic flux of heat and VD on the flow of magnetohydrodynamics via a canal vertically with heat generation [20].

In this work, the influences of VD and JH on radiative MHD flow through parallel porous plates, which were analyzed in the existence of oscillatory suction and injection, were examined. The study was carried out theoretically via the NFD (numerical finite difference) technique, and the findings were verified using the analytical eigenfunction expansion technique for special cases. While several studies have separately addressed the impacts of Joule heating, viscous dissipation, radiation, and oscillatory suction/injection on MHD flows, limited attention has been given to their combined effect in a confined channel between parallel porous plates under both a moving boundary and a constant pressure gradient. Moreover, most existing works focus on steady or non-oscillatory boundary conditions, neglecting the dynamic influence of periodic suction/injection on the thermal and flow fields. This study addresses these gaps by analyzing an unsteady MHD flow between porous plates with a moving upper boundary, accounting simultaneously for Joule heating, viscous dissipation, radiative heat transfer, and oscillatory suction/injection. This integrated approach offers new insights relevant to advanced thermal systems, such as porous heat exchangers, MHD pumps, and filtration devices involving electrically conducting fluids.

2. MATHEMATICAL MODELING

Considering a transient MHD developed fully laminar flow of an incompressible viscous fluid passing into a canal restricted by two infinitely non-conducting porous plates with a distance h between them. Initially, the plates are stationary and have a surrounding temperature of T_0. When $t > 0$, the top plate gained a U_0 (velocity) while the lower plate was stationary, and the lower and top plates were sustained at two constant temperatures ($Tw1$ and $Tw2$), respectively. The fluid is acted upon by the motion of the top plate and a constant pressure gradient $\partial p/\partial x$ in the x trend with oscillatory suction and injection $V(t) = V_0(1 + \epsilon\cos(\omega^* t))$.

The channel undergoes a normal magnetic field B_0. The viscous heating, heat generation, Joule heating, and radiation effects are considered in the physical model shown in Figure 1. By assuming Boussinesq's approximation with constant fluid properties, the unstable two-dimensional boundary layer flow can be proven by the following formulas:

$$\frac{\partial u^*}{\partial t^*} + \mathrm{v}(t)\frac{\partial u^*}{\partial y^*} = -\frac{1}{\rho}\frac{\partial p^*}{\partial x^*} + \nu\frac{\partial^2 u^*}{\partial y^{*2}} - \frac{\sigma B_0^2}{\rho}u^* \tag{1}$$

$$\frac{\partial T}{\partial t^*} + \mathrm{v}(t)\frac{\partial T}{\partial y^*} = \frac{k}{\rho c_p}\frac{\partial^2 \mathrm{T}}{\partial y^{*2}} + \frac{\nu}{c_p}\left(\frac{\partial u^*}{\partial y^*}\right)^2 + \sigma B_0^2 u^{*2} - \frac{\partial q_r}{\partial y^*} + \frac{Q_0}{\rho c_p}(\mathrm{T} - T_{\mathrm{w1}}) \tag{2}$$

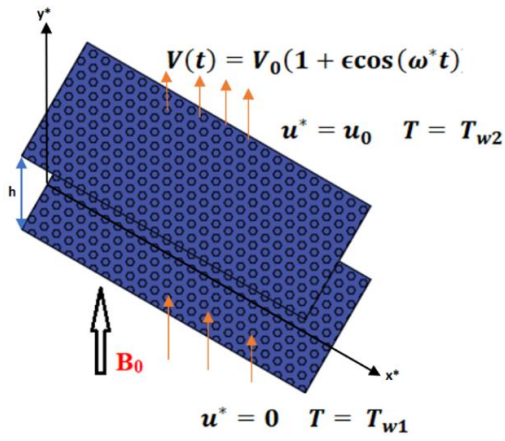

Figure 1. Physical model description

The considered primary and boundary conditions (BCs) are:

$$\begin{gathered} t^* \le 0: u^* = 0, T = T_{w1}, 0 \le y^* \le h \\ t^* > 0: u^* = 0, T = T_{w1}, \text{at } y^* = 0 \\ u^* = u_0, T = T_{w2}, at\ y^* = h \end{gathered} \tag{3}$$

When radiation is estimated via the Rosseland approximation, the radiative heat flux is

$$q_r = \frac{-4\sigma^*}{3k^*}\frac{\partial T^4}{\partial y^*} \tag{4}$$

Using Taylor series expansion for T^4, then

$$\frac{\partial T^4}{\partial y^*} \cong 4T_0^3\frac{\partial T}{\partial y^*} \tag{5}$$

And then

$$\frac{\partial q_r}{\partial y^*} = -\frac{16\sigma^*}{3k^*}T_0^3\frac{\partial^2 T}{\partial y^{*2}} \tag{6}$$

Using Eq. (5), Eq. (2) becomes

$$\frac{\partial T}{\partial t^*} + \mathrm{v}(t)\frac{\partial T}{\partial y^*} = \frac{k}{\rho c_p}\left(1 + \frac{16\sigma^*}{3kk^*}T_0^3\right)\frac{\partial^2 T}{\partial y^{*2}} + \frac{\nu}{c_p}\left(\frac{\partial u^*}{\partial y^*}\right)^2 + \sigma B_0^2 u^{*2} + \frac{Q_0}{\rho c_p}(\mathrm{T} - T_{\mathrm{w1}}) \tag{7}$$

where, υ, T and k are kinematic viscosity, fluid temperature, and thermal conductivity, respectively. u^* and c_p are axial velocity and specific heat, respectively.

The governing equations (GEs) are given in dimensionless form using the next dimensionless variables:

$$\begin{gathered} x = \frac{x^*}{h}, y = \frac{y^*}{h}, t = \frac{\nu t^*}{h^2}, \omega = \frac{h^2\omega^*}{\nu} \\ u = \frac{u^*}{u_0}, \theta = \frac{T - T_{w1}}{T_{w2} - T_{w1}}, p = \frac{hp^*}{\mu u_0} \end{gathered} \tag{8}$$

The dimensionless equations become:

$$\frac{\partial u}{\partial t} + S(1 + \epsilon\cos(\omega t))\frac{\partial u}{\partial y} = -\frac{\partial p}{\partial x} + \frac{\partial^2 u}{\partial y^2} - Mu \tag{9}$$

$$\frac{\partial\theta}{\partial t}+S(1+\epsilon\cos(\omega t))\frac{\partial\theta}{\partial y} = \frac{(1+R)}{Pr}\frac{\partial^2\theta}{\partial y^2}+E_c\left(\frac{\partial u}{\partial y}\right)^2+ME_cu^2+Q\theta \quad (10)$$

where,

$$M=\frac{\sigma B_0^2h^2}{\mu},\ E_c=\frac{{u_0}^2}{c_p(T_{w2}-T_{w1})},\ Pr=\frac{\mu c_p}{k}$$
$$R=\frac{16\sigma^*T_0^3}{3kk^*},\ Q=\frac{Q_0h^2}{\mu c_p},\ S=\frac{hV_0}{\nu}$$

The corresponding dimensionless BCs are
Initially,

$$t\le 0:\ u=0,\ \theta=0,\ \text{for all y}$$
$$t>0:\ u=0,\quad \theta=0,\quad \text{at } y=0$$
$$u=1,\quad \theta=1,\quad \text{as } y=1$$

In formulating the governing equations, the Boussinesq approximation is employed to account for buoyancy effects without introducing significant complexity, which is valid for small temperature differences typically encountered in such flows. The Rosseland approximation used for radiative heat flux assumes that the fluid medium is optically thick, typically valid when the optical thickness $\tau \gg 1$. This condition implies that radiative energy is diffused across the medium rather than directly transmitted. While this assumption is commonly adopted for thermal MHD flows in dense or particulate-laden fluids, its accuracy may diminish in optically thin media. However, for the moderately absorbing fluid and channel geometry considered here, the approximation offers a practical simplification without significantly compromising accuracy. Fluid properties are considered constant, which is a reasonable assumption for low to moderate temperature variations in incompressible MHD flows with weak thermal gradients.

3. NUMERICAL ANALYSIS

Eqs. (9) and (10) with their initial and BCs are numerically solved using the finite-difference Crank-Nicolson method, an implicit numerical technique that produces accurate results. In this method, the forward finite difference approximation represents the derivatives in the time domain, while the central finite difference approximation represents the derivatives in the spatial domain.

$$\frac{\partial u}{\partial t}=\frac{u_i^{n+1}-u_i^n}{\Delta t} \quad (11)$$

$$\frac{\partial^2 u}{\partial y^2}=\frac{(u_{i+1}-2u_i+u_{i-1})}{(\Delta y)^2}$$
$$\frac{\partial\theta}{\partial t}=\frac{\theta_i^{n+1}-\theta_i^n}{\Delta t} \quad (12)$$
$$\frac{\partial^2\theta}{\partial y^2}=\frac{(\theta_{i+1}-2\theta_i+\theta_{i-1})}{(\Delta y)^2}$$

The indexed variable *i* represents the point location in the y direction, while *n* represents the time level. The step sizes Δy = 0.01 and Δt = 0.01 are taken in the discretization domain.

The following formulas transform the dimensionless governing equations into the following finite difference equations.

$$\frac{u_i^{n+1}-u_i^n}{\Delta t}+\mathrm{S}(1+\epsilon\cos(\omega t^{n+1}))\frac{u_{i+1}^n-u_i^n}{\Delta y}=-\frac{dp}{dx} +\frac{(u_{i+1}^{n+1}-2u_i^{n+1}+u_{i-1}^{n+1})+(u_{i+1}^n-2u_i^n+u_{i-1}^n)}{2(\Delta y)^2} -\frac{M}{2}(u_i^{n+1}+u_i^n) \quad (13)$$

$$\frac{\theta_i^{n+1}-\theta_i^n}{\Delta t}+\mathrm{S}(1+\epsilon\cos(\omega t^{n+1}))\frac{\theta_{i+1}^n-\theta_i^n}{\Delta y}= \frac{(1+\mathrm{R})}{2Pr}\left[\frac{(\theta_{i+1}^{n+1}-2\theta_i^{n+1}+\theta_{i-1}^{n+1})+(\theta_{i+1}^n-2\theta_i^n+\theta_{i-1}^n)}{(\Delta y)^2}\right]+E_c\left[\frac{u_{i+1}^n-u_i^n}{\Delta y}\right]^2+ \mathrm{M}E_cu_i^{n+1}+\frac{Q}{2}(\theta_i^{n+1}+\theta_i^n) \quad (14)$$

Then, Eqs. (13) and (14) are converted to the following implicit form

$$u_{i-1}^{n+1}+d1u_i^{n+1}+u_{i+1}^{n+1}=\mathrm{b1} \quad (15)$$

$$\theta_{i-1}^{n+1}+d2\theta_i^{n+1}+\theta_{i+1}^{n+1}=b2 \quad (16)$$

where,

$$\mathrm{d1}=-2\left[1+\frac{(\Delta y)^2}{\Delta t}+\frac{M(\Delta y)^2}{2}\right]$$
$$\mathrm{b1}=-2\Delta y\frac{dp}{dx}+2(\Delta y)^2\mathrm{S}(1+\epsilon\cos(\omega t^{n+1}))(u_{i+1}^n-u_i^n) -\frac{2(\Delta y)^2}{\Delta t}u_i^n-(u_{i+1}^n-2u_i^n+u_{i-1}^n)+M(\Delta y)^2u_i^n$$
$$d2=\frac{Pr(\Delta y)^2Q}{(1+R)}-\frac{2Pr(\Delta y)^2}{\Delta t(1+R)}-2$$
$$b2=-\frac{2Pr(\Delta y)^2}{(1+R)}\left\{\frac{\theta_i^n}{\Delta t}-\mathrm{S}(1+\epsilon\cos(\omega t^{n+1}))\frac{\theta_i^{n+1}-\theta_i^n}{\Delta y}+ \frac{(1+\mathrm{R})(\theta_{i+1}^n-2\theta_i^n+\theta_{i-1}^n)}{2Pr(\Delta y)^2}+E_c\left[\frac{u_{i+1}^n-u_i^n}{\Delta y}\right]^2+\mathrm{M}E_cu_i^n+\frac{Q}{2}\theta_i^n\right\}$$

Eqs. (15) and (16) constitute a tridiagonal system of equations at the time level (n + 1) that are solved for the velocity **u** and temperature **θ** using the Thomas algorithm and depending on the values at time level n.

The Crank-Nicolson method used in this study is unconditionally stable for linear problems and conditionally stable for nonlinear problems, which was carefully accounted for in our implementation. The convergence of the solution was verified through iterative residual checks at each time step. Additionally, a grid independence test was conducted by comparing results for different mesh sizes. It was observed that further refinement caused negligible change (< 1%) in velocity and temperature profiles, justifying the chosen step sizes (Δy = 0.01, Δt = 0.01) as an optimal balance between accuracy and computational cost.

4. ANALYTICAL SOLUTION

The solution of numerical has been verified by contrasting it with the analytical solution under particular conditions. The equations for momentum and energy are solved using the eigenfunction expansion technique.

4.1 Velocity solution

A negligible S parameter is used to solve the velocity equation analytically.

$$\frac{\partial u}{\partial t} = -\frac{dp}{dx} + \frac{\partial^2 u}{\partial y^2} - \mathrm{Mu} \tag{17}$$

The corresponding BCs are
When

$$\begin{gathered} t \le 0: u = 0, \text{ For all y} \\ t > 0: u = 0, \quad \text{at } y = 0 \\ u = 1, \quad \text{at } y = 1 \end{gathered} \tag{18}$$

To apply the eigenfunction expansion method, the BCs must be transformed into homogeneous, linear equations. Consequently, the variable that follows is presented:

$$H_1(y,t) = u(y,t) - \mathrm{y} \tag{19}$$

Therefore, the velocity equation will be:

$$\frac{\partial H_1}{\partial t} = \frac{\partial^2 H_1}{\partial y^2} - \mathrm{M}H_1 - \mathrm{My} - \frac{dp}{dx} \tag{20}$$

Below are the corresponding BCs
When

$$\begin{gathered} t \le 0: H_1 = -y, \text{ For all values of y} \\ t > 0: H_1 = 0, \quad \text{at } y = 0 \\ H_1 = 0, \quad \text{at } y = 1 \end{gathered} \tag{21}$$

Let $H_1(y,t) = \phi_1(y)a_1(t)$.
By replacing the function $H_1(y, t)$ and its derivatives into the homogeneous form of Eq. (20), the eigenvalue problem can be found.

$$\begin{gathered} \frac{d^2\phi_1}{dy^2} + \lambda\phi_1 = 0, \phi_1(0) = \phi_1(1) = 0 \\ \frac{da_1}{dt} + (M + \lambda)a_1 = 0 \end{gathered} \tag{22}$$

The eigenvalue problem solution is:

$$\phi_{1n}(y) = sin\left(\sqrt{\lambda_{1n}}y\right) \tag{23}$$

And the eigenvalues are:

$$\lambda_{1n} = (n\pi)^2 \tag{24}$$

where, n = 1, 2, 3, ..., ∞.
Then, the solution of $H_1(y,t)$ is coming as:

$$H_1(y,t) = \sum_{n=1}^{\infty} a_{1n}(t)\, sin\left(\sqrt{\lambda_{1n}}y\right)$$

By substituting $H_1(y,t)$ into the nonhomogeneous Eq. (20), the solution of $a_{1n}(t)$ is

$$\begin{gathered} a_{1n}(t) = a_{1n}(0)e^{-(M+\lambda_{1n})t} \\ + \frac{2\left[-\frac{dp}{dx} + (\frac{dp}{dx} + M)(-1)^n\right]}{n\pi(M+\lambda_{1n})}\left[1 - e^{-(M+\lambda_{1n})t}\right] \end{gathered} \tag{25}$$

By applying the initial condition

$$H_1(y,0) = -\mathrm{y}$$

Then $a_{1n}(0) = \frac{2(-1)^n}{n\pi}$.
Finally, the dimensionless velocity will take the form:

$$u(y,t) = y + \sum_{n=1}^{\infty}\left\{\frac{2(-1)^n}{n\pi}e^{-(M+\lambda_{1n})t} + \frac{2\left[-\frac{dp}{dx} + (\frac{dp}{dx} + M)(-1)^n\right]}{n\pi(M+\lambda_{1n})}\left[1 - e^{-(M+\lambda_{1n})t}\right]\right\} sin(n\pi y)$$

4.2 Temperature solution

The analytical solution to the energy equation involves the use of negligible Ec and S parameters.

$$\frac{\partial\theta}{\partial t} = \frac{(1+R)}{Pr}\frac{\partial^2\theta}{\partial y^2} + \mathrm{Q}\theta \tag{26}$$

The corresponding BCs are
When

$$\begin{gathered} t \le 0: \theta = 0, \text{ for all y} \\ t > 0: \theta = 0, \quad \text{at } y = 0 \\ \theta = 1, \quad \text{at } y = 1 \end{gathered} \tag{27}$$

The boundary conditions must be transformed into homogeneous, linear equations to use the eigenfunction expansion approach. Consequently, the subsequent variable is presented:

$$H_2(y,t) = \theta(y,t) - \mathrm{y} \tag{28}$$

Then, the energy equation will be:

$$\frac{\partial H_2}{\partial t} = \frac{(1+R)}{Pr}\frac{\partial^2 H_2}{\partial y^2} + \mathrm{Q}H_2 + \mathrm{Qy} \tag{29}$$

The corresponding BCs are listed below:
When

$$\begin{gathered} t \le 0: H_2 = -y, \text{ For all values of y} \\ t > 0: H_2 = 0, \quad \text{at } y = 0 \\ H_2 = 0, \quad \text{at } y = 1 \end{gathered} \tag{30}$$

Let

$$H_2(y,t) = \phi_2(y)a_2(t)$$

The eigenvalue problem can be obtained by replacing the function $H_2(y,t)$ and its derivatives with the homogeneous part of Eq. (29).

$$\begin{gathered} \frac{d^2\phi_2}{dy^2} + \lambda\phi_2 = 0, \phi_2(0) = \phi_2(1) = 0 \\ \frac{da_2}{dt} + \left(\frac{(1+R)}{Pr}\lambda - Q\right)a_2 = 0 \end{gathered} \tag{31}$$

The solution of the eigenvalue problem is:

$$\phi_{2n}(y) = sin\left(\sqrt{\lambda_{2n}}y\right) \tag{32}$$

The eigenvalues are:

$$\lambda_{2n} = (n\pi)^2 \tag{33}$$

where, n = 1, 2, 3, ..., ∞.

Then, the solution of $H_2(y,t)$ is coming as:

$$H_2(y,t) = \sum_{n=1}^{\infty} a_{2n}(t)\, sin\left(\sqrt{\lambda_{2n}}y\right)$$

By replacing $H_2(y,t)$ into the nonhomogeneous Eq. (29), then the time-dependent function $a_{2n}(t)$ solution is

$$a_{2n}(t) = a_{2n}(0)e^{-\left(\frac{(1+R)}{Pr}\lambda_{2n}-Q\right)t} - \frac{2Q(-1)^n}{n\pi\left(\frac{(1+R)}{Pr}\lambda_{2n}-Q\right)}\left[1-e^{-\left(\frac{(1+R)}{Pr}\lambda_{2n}-Q\right)t}\right] \tag{34}$$

By utilizing the condition:

$$H_2(y,0) = -y$$

Then $a_{2n}(0) = \frac{2(-1)^n}{n\pi}$.

Lastly, the following solution has been used for the dimensionless temperature.

$$\theta(y,t) = y + \sum_{n=1}^{\infty}\left\{\frac{2(-1)^n}{n\pi}e^{-\left(\frac{(1+R)}{Pr}\lambda_{2n}-Q\right)t} - \frac{2Q(-1)^n}{n\pi\left(\frac{(1+R)}{Pr}\lambda_{2n}-Q\right)}\left[1-e^{-\left(\frac{(1+R)}{Pr}\lambda_{2n}-Q\right)t}\right]\right\} sin(n\pi y)$$

5. RESULTS AND DISCUSSION

The impacts of injection, radiation, heat source, viscous dissipation, magnetic flux, Joule heating, oscillatory suction, and heat transfer over a horizontal channel are examined in this work. Graphic representations of the **θ** (temperature profile) and u (velocity profile) are provided for various **M** (magnetic parameter), **R** (radiation parameter), **Ec** (Eckert number), **Q** (heat-generating parameter), **S** (suction parameter), **Pr** (Prandtl number), and **ωt** (frequency parameter) values.

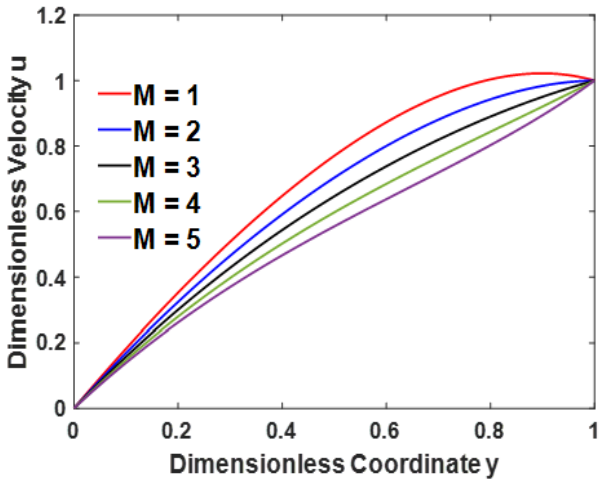

Figure 2. Impact of **M** (magnetic parameter) on **u**

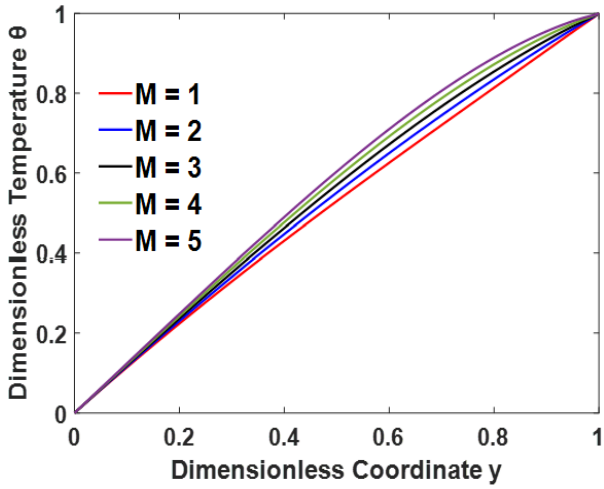

Figure 3. Impact of **M** on **θ**

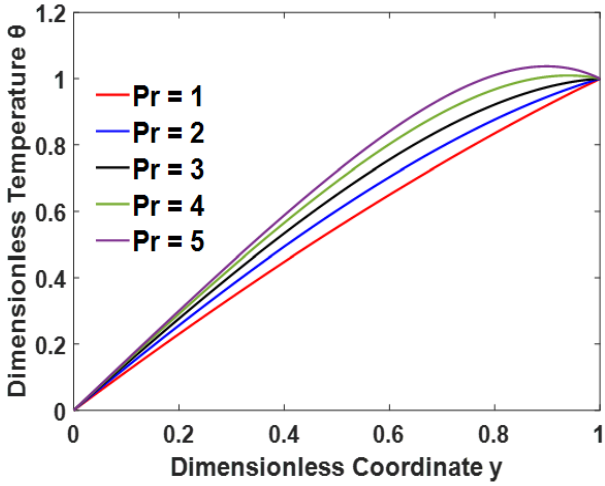

Figure 4. Impact of **Pr** on **θ**

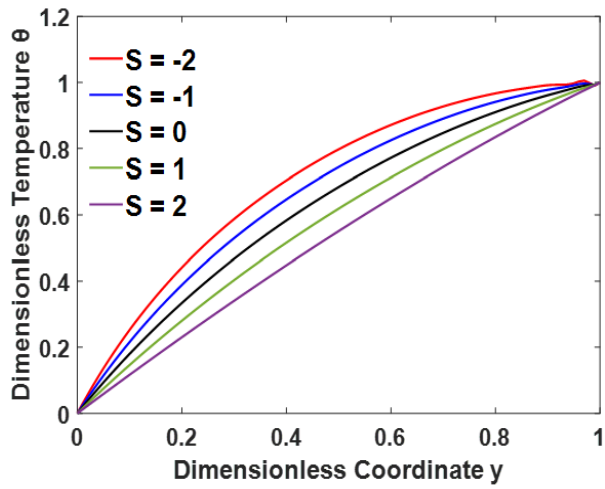

Figure 5. Impact of **S** (suction parameter) on **θ**

Figure 2 displays the impact of **M** on **u.** It is shown that the fluid flow slows down as the **M** rises. When the transverse MF is applied to the channel, the Lorentz force is created, which resists the flow and causes the flow to be retarded. The impacts of M on the **θ**, Figure 3. It is demonstrated that the temperature rises as the **M** increases. This is because energy is produced while the walls are maintained at a steady temperature and in

slow motion.

The impact of the **Pr** on the θ is displayed in Figure 4. It is detected that when the **Pr** rises, the θ also increases. This results from heat building up due to viscous dissipation, raising temperature readings.

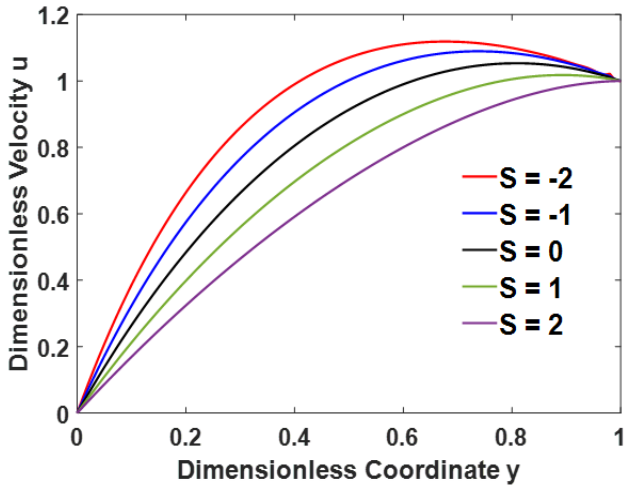

Figure 6. Impact of **S** on **u**

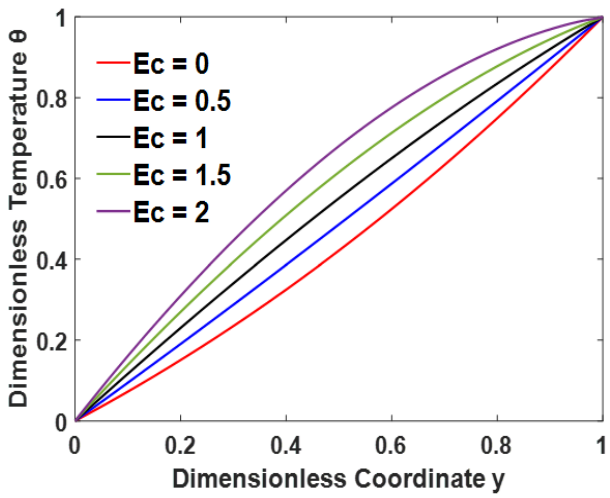

Figure 7. Impact of **Ec** (Eckert number) on **θ**

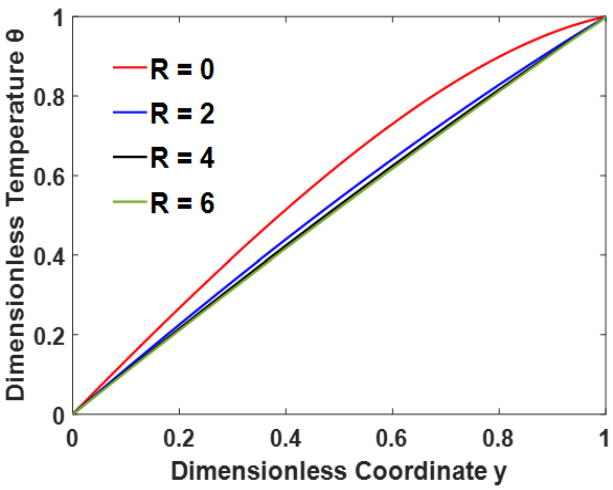

Figure 8. Impact of **R** (radiation parameter) on **θ**

Figures 5 and 6 depict the impact of **S** on temperature and velocity distributions. When **S** increases, **u** and **θ** values decrease. This is because the heated fluid particles move toward the surroundings and are replaced by cold fluid particles, causing the fluid to slow down and reduce temperature values.

Figure 7 illustrates how the **Ec** affects temperature. When the viscous dissipation effect increases, so does the temperature. This occurs because the interactions between its particles raise the fluid's internal energy and temperature. Figure 8 illustrates how the R affects the temperature distribution. It demonstrates that as the radiation parameter values increase, the temperature drops.

Figure 9 shows the **θ** for numerous values of the **Q**. As **Q** increases, **θ** values rise due to increased heat generation. This effect results from increased convection rates brought on by heat generation.

Figures 10 and 11 display the **u** and **θ** at various values of the **ωt**, which spans from 0 to π. The **u** and **θ** values increase as the **ωt** value increases.

Figure 12 shows the transient velocity at different locations. The transient velocity profile has a periodic pattern due to periodic suction or injection.

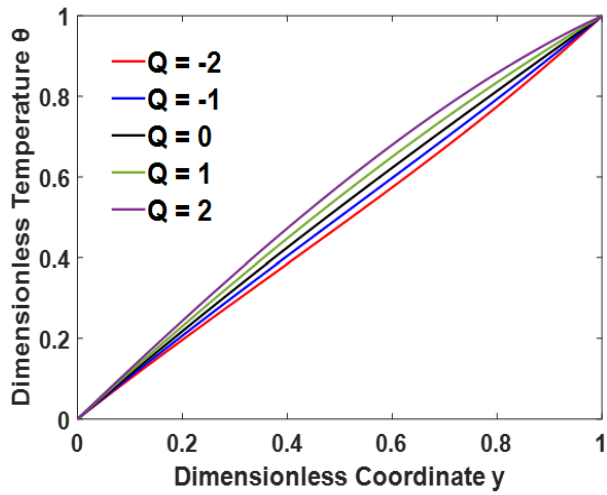

Figure 9. Impact of heat generating parameter **Q** on **θ**

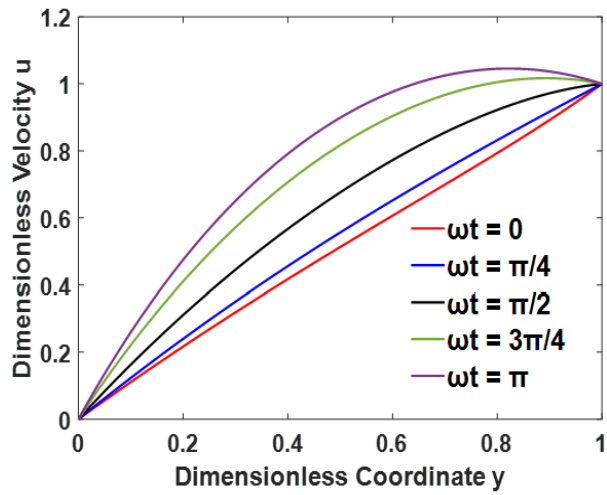

Figure 10. Impact of frequency parameter **ωt** on **u**

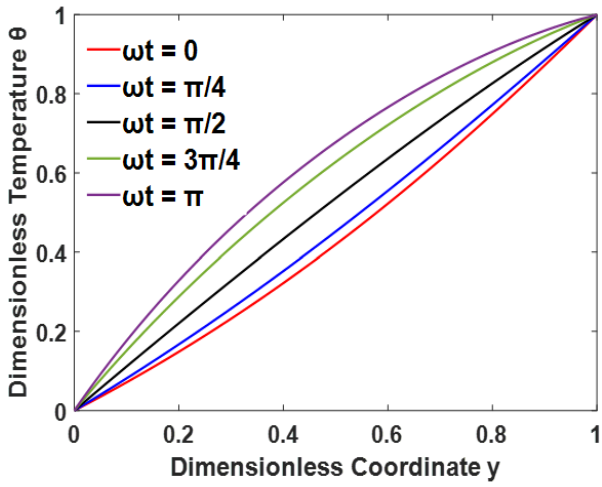

Figure 11. Impact of **ωt** on **θ**

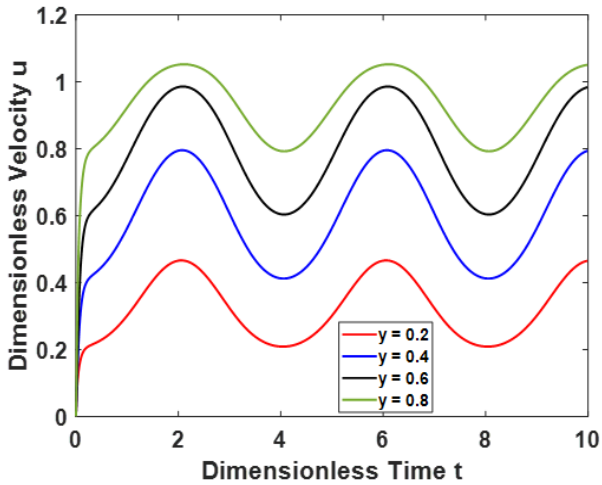

Figure 12. Transient velocity at different locations

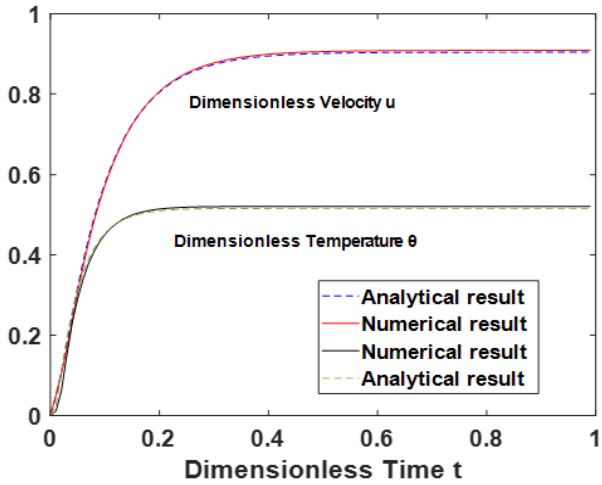

Figure 13. Numerical and analytical results for velocity and temperature profiles

The increase in fluid temperature with the Eckert number is due to enhanced viscous dissipation, where mechanical energy is irreversibly converted into internal energy (heat) within the fluid, leading to temperature rise. In contrast, a higher radiation parameter indicates stronger radiative heat transfer from the fluid to the surroundings, which acts as a thermal sink, thereby reducing the fluid temperature. Regarding suction/injection, the periodic mass exchange through the porous plates introduces oscillatory momentum and thermal disturbances. When combined with the magnetic field, the Lorentz force generated opposes fluid motion, modifying the phase and amplitude of velocity and temperature profiles. This interaction can dampen or amplify flow oscillations depending on the frequency and strength of the suction relative to magnetic resistance. Such coupling significantly influences transient thermal response and energy transport in the system.

Excellent agreement is discovered when comparing the numerical results for particular circumstances with the results produced by the analytical approach, as shown in Figure 13 and Table 1.

Table 1. Comparison of numerical and analytical techniques

Time	Velocity		Temperature	
	Numerical Result	Analytical Result	Numerical Result	Analytical Result
0.1	0.5319	0.5386	0.4326	0.4372
0.2	0.7938	0.7924	0.5127	0.5085
0.3	0.8737	0.8700	0.5202	0.5152
0.4	0.8981	0.8937	0.5209	0.5158
0.5	0.9055	0.9009	0.5209	0.5159

6. CONCLUSIONS

This study presents a detailed analysis of unsteady radiative MHD flow between parallel porous plates under the combined effects of Joule heating, viscous dissipation, and oscillatory suction/injection. The velocity and temperature fields were obtained using both numerical (Crank-Nicolson method) and analytical (eigenfunction expansion) techniques, with excellent agreement observed for specific cases. Key findings include:

(a) Fluid temperature increases with Joule heating, viscous dissipation, and the Eckert number, but decreases with stronger radiation and suction effects.
(b) The magnetic field suppresses fluid motion while enhancing thermal energy due to Joule heating.
(c) Periodic suction/injection introduces oscillations in both flow and temperature profiles, which are influenced by magnetic damping.
(d) The relative contributions of Joule heating and viscous dissipation vary depending on magnetic field strength and velocity gradients, highlighting the importance of parameter interplay in heat generation mechanisms.

These results are applicable to thermal control in MHD-based engineering systems, such as heat exchangers with porous media, MHD pumps, filtration devices, and geophysical flows where thermal and electromagnetic interactions play a role. The model can be extended to three-dimensional or axisymmetric flows. Further research may incorporate nonlinear radiation models, temperature-dependent properties, or spatially varying magnetic fields to enhance realism and broaden applicability.

REFERENCES

[1] Jha, B.K., Ajibade, A.O. (2009). Free convective flow of heat generating/absorbing fluid between vertical porous plates with periodic heat input. International

Communications in Heat and Mass Transfer, 36(6): 624-631. https://doi.org/10.1016/j.icheatmasstransfer.2009.03.003

[2] Wahiduzzaman, M., Islam, M.T., Sultana, P., Afikuzzaman, M. (2014). MHD Couette flow of a Casson fluid between parallel porous plates. Progress in Nonlinear Dynamics and Chaos, 2(2): 51-60.

[3] Palani, G., Gnanambigai, J. (2014). Theoretical solution of impulsively started vertical porous plate with variable temperature under the influence of magnetic field and thermal radiation. Journal of Engineering Thermophysics, 23(2): 129-136. https://doi.org/10.1134/S1810232814020052

[4] Maleki, H., Safaei, M.R., Alrashed, A.A., Kasaeian, A. (2019). Flow and heat transfer in non-Newtonian nanofluids over porous surfaces. Journal of Thermal Analysis and Calorimetry, 135(3): 1655-1666. https://doi.org/10.1007/s10973-018-7277-9

[5] Fagbade, A.I., Falodun, B.O., Omowaye, A.J. (2018). MHD natural convection flow of viscoelastic fluid over an accelerating permeable surface with thermal radiation and heat source or sink: Spectral homotopy analysis approach. Ain Shams Engineering Journal, 9(4): 1029-1041. https://doi.org/10.1016/j.asej.2016.04.021

[6] Nandi, S., Kumbhakar, B. (2020). Unsteady MHD free convective flow past a permeable vertical plate with periodic movement and slippage in the presence of Hall current and rotation. Thermal Science and Engineering Progress, 19: 100561. https://doi.org/10.1016/j.tsep.2020.100561

[7] Ajibade, A.O., Umar, A.M., Kabir, T.M. (2021). An analytical study on effects of viscous dissipation and suction/injection on a steady MHD natural convection Couette flow of heat generating/absorbing fluid. Advances in Mechanical Engineering, 13(5): 16878140211015862. https://doi.org/10.1177/16878140211015862

[8] Krishna, M.V., Reddy, M.G., Chamkha, A.J. (2021). Heat and mass transfer on unsteady MHD flow through an infinite oscillating vertical porous surface. Journal of Porous Media, 24(1): 81-100. https://doi.org/10.1615/JPorMedia.2020025021

[9] Ahammad, N.A., Badruddin, I.A., Kamangar, S., Khaleed, H.M.T., Saleel, C.A., Mahlia, T.M.I. (2021). Heat transfer and entropy in a vertical porous plate subjected to suction velocity and MHD. Entropy, 23(8): 1069. https://doi.org/10.3390/e23081069

[10] Loganathan, A., Elamparithi, S. (2023). MHD heat and mass transfer steady flow of a convective fluid through a porous plate in the presence of multiple parameters along with Dufour effect. International Journal of Heat and Technology, 41(1): 205-212. https://doi.org/10.18280/ijht.410122

[11] Alim, M.A.A., Alam, M.M., Al-Mamun, A. (2007). Joule heating effect on the coupling of conduction with magnetohydrodynamic free convection flow from a vertical flat plate. Nonlinear Analysis: Modelling and Control, 12(3): 307-316. https://doi.org/10.15388/NA.2007.12.3.14688

[12] Abo-Eldahab, E.M., El Aziz, M.A. (2005). Viscous dissipation and Joule heating effects on MHD-free convection from a vertical plate with power-law variation in surface temperature in the presence of Hall and ion-slip currents. Applied Mathematical Modelling, 29(6): 579-595. https://doi.org/10.1016/j.apm.2004.10.005

[13] Das, S., Jana, R.N., Makinde, O.D. (2015). Magnetohydrodynamic mixed convective slip flow over an inclined porous plate with viscous dissipation and Joule heating. Alexandria Engineering Journal, 54(2): 251-261. https://doi.org/10.1016/j.aej.2015.03.003

[14] Jaber, K.K. (2014). Effects of viscous dissipation and Joule heating on MHD flow of a fluid with variable properties past a stretching vertical plate. European Scientific Journal, 10(33): 383-393.

[15] Shamshuddin, M.D., Satya Narayana, P.V. (2020). Combined effect of viscous dissipation and Joule heating on MHD flow past a Riga plate with Cattaneo–Christov heat flux. Indian Journal of Physics, 94(9): 1385-1394. https://doi.org/10.1007/s12648-019-01576-7

[16] Sharma, B.K., Gandhi, R. (2022). Combined effects of Joule heating and non-uniform heat source/sink on unsteady MHD mixed convective flow over a vertical stretching surface embedded in a Darcy-Forchheimer porous medium. Propulsion and Power Research, 11(2): 276-292. https://doi.org/10.1016/j.jppr.2022.06.001

[17] Pal, D., Talukdar, B. (2011). Combined effects of Joule heating and chemical reaction on unsteady magnetohydrodynamic mixed convection of a viscous dissipating fluid over a vertical plate in porous media with thermal radiation. Mathematical and Computer Modelling, 54(11-12): 3016-3036. https://doi.org/10.1016/j.mcm.2011.07.030

[18] Tarakaramu, N., Narayana, P.V.S., Babu, D.H., Sarojamma, G., Makinde, O.D. (2021). Joule heating and dissipation effects on magnetohydrodynamic couple stress nanofluid flow over a bidirectional stretching surface. International Journal of Heat and Technology, 39(1): 205-212. https://doi.org/10.18280/ijht.390122

[19] Khan, M.S., Siddiqui, M.A., Afridi, M.I. (2022). Finite difference simulation of nonlinear convection in magnetohydrodynamic flow in the presence of viscous and Joule dissipation over an oscillating plate. Symmetry, 14(10): 1988. https://doi.org/10.3390/sym14101988

[20] Abdullah, M. (2024). Effects of viscous dissipation and periodic heat flux on MHD free convection channel flow with heat generation. Frontiers in Heat and Mass Transfer, 22(1): 141-156. https://doi.org/10.32604/fhmt.2024.046788

NOMENCLATURE

$a_{1,2}$	separation variables
B_0	magnetic flux density, T
C_p	specific heat, $J \cdot kg^{-1} \cdot K^{-1}$
E_c	Eckert number
k	thermal conductivity, $W \cdot m^{-1} \cdot K^{-1}$
M	magnetic parameter
p*	pressure, pa
p	nondimensional pressure
P_r	Prandtl number
q_r	radiative heat flux, $W \cdot m^{-2}$
Q_0	heat generation coefficient
Q	heat generating parameter
R	radiation parameter

S	suction parameter
T	temperature, K
$T_{w1,2}$	plates temperatures, K
t^*	time, s
t	nondimensional time
u^*	velocity, $m \cdot s^{-1}$
u	nondimensional velocity
x^*, y^*	Cartesian coordinates, m
x, y	nondimensional coordinates

Greek symbols

$\phi_{1,2}$	separation variables
$\boldsymbol{\theta}$	nondimensional temperature
$\lambda_{1,2}$	separation constants
υ	kinematic viscosity, $m^2 \cdot s^{-1}$
ρ	density, $kg \cdot m^{-3}$
σ	electrical conductivity, siemens m^{-1}
ω^*	frequency of suction velocity oscillation, $rad \cdot s^{-1}$
ω	frequency parameter